Opposing roles of NF-κB in anti-cancer treatment outcome unveiled by cross-species investigations

Hua Jing,[1,5] Julia Kase,[2,5] Jan R. Dörr,[2] Maja Milanovic,[2] Dido Lenze,[3] Michael Grau,[4] Gregor Beuster,[1] Sujuan Ji,[2] Maurice Reimann,[2] Peter Lenz,[4] Michael Hummel,[3] Bernd Dörken,[1,2] Georg Lenz,[2] Claus Scheidereit,[1] Clemens A. Schmitt,[1,2,6] and Soyoung Lee[2]

[1]Max-Delbrück-Center for Molecular Medicine, 13125 Berlin, Germany; [2]Department of Hematology, Oncology, and Tumor Immunology, Charité-Universitätsmedizin, Campus Virchow Clinic, Molekulares Krebsforschungszentrum, D-13353 Berlin, Germany; [3]Department of Pathology, Charité-Universitätsmedizin, D-10117 Berlin, Germany; [4]Department of Physics, Philipps-University Marburg, D-35032 Marburg, Germany

In malignancies, enhanced nuclear factor-κB (NF-κB) activity is largely viewed as an oncogenic property that also confers resistance to chemotherapy. Recently, NF-κB has been postulated to participate in a senescence-associated and possibly senescence-reinforcing cytokine response, thereby suggesting a tumor-restraining role for NF-κB. Using a mouse lymphoma model and analyzing transcriptome and clinical data from lymphoma patients, we show here that therapy-induced senescence presents with and depends on active NF-κB signaling, whereas NF-κB simultaneously promotes resistance to apoptosis. Further characterization and genetic engineering of primary mouse lymphomas according to distinct NF-κB-related oncogenic networks reminiscent of diffuse large B-cell lymphoma (DLBCL) subtypes guided us to identify Bcl2-overexpressing germinal center B-cell-like (GCB) DLBCL as a clinically relevant subgroup with significantly superior outcome when NF-κB is hyperactive. Our data illustrate the power of cross-species investigations to functionally test genetic mechanisms in transgenic mouse tumors that recapitulate distinct features of the corresponding human entity, and to ultimately use the mouse model-derived genetic information to redefine novel, clinically relevant patient subcohorts.

Initially identified by their interaction with immunoglobulin enhancer sequences, nuclear factor-κB (NF-κB) transcription factors control the expression of a large set of target genes, thereby orchestrating a plethora of biological functions, including cell survival, inflammation, and immunity (Sen and Baltimore 1986; Hayden and Ghosh 2008). Specifically, cancer-relevant properties such as suppression of apoptosis, growth promotion, enhanced migration, and invasiveness have been attributed to NF-κB signaling (Ben-Neriah and Karin 2011). Activating mutations in NF-κB transcription factors or their upstream signaling components are common findings in various lymphoma entities (Lenz et al. 2008a; Compagno et al. 2009; for review, see also Staudt 2010 and references therein). Although oncogenic mutations in NF-κB signal mediators appear to be rare in solid tumors, oncogenic

signaling may enhance NF-κB activity in the absence of mutations, as inflammation-associated NF-κB-driven cytokine production promotes carcinogenesis in a non-cell-autonomous fashion (Staudt 2010; Ben-Neriah and Karin 2011). Accordingly, mouse models demonstrated an oncogenic role for NF-κB in the development of lymphomas and solid tumors (Basseres et al. 2010; Calado et al. 2010; Yang et al. 2010). However, other mouse model-based studies found NF-κB transcription factors or upstream activators rather to act as tumor suppressors (Luedde et al. 2007; Keller et al. 2010), thereby underscoring the complexity and potential context dependency of NF-κB network-mediated effector functions (Perkins and Gilmore 2006). Indeed, NF-κB has been shown to mediate or, conversely, block apoptosis in different settings (Wang et al. 1998; Ryan et al. 2000), and non-cell-autonomous components of NF-κB action may further add to the diverse roles NF-κB apparently plays in tumor development.

Activation of NF-κB also occurs in response to DNA damage (Brach et al. 1991; Stilmann et al. 2009; Hinz et al. 2010), the mode by which most conventional chemother-

apeutic agents exert their anti-cancer activity. Enhanced anti-tumor efficacy has been observed following inhibition of NF-κB function and was primarily linked to NF-κB-mediated suppression of apoptosis as the chemoresistance-underlying mechanism (Wang et al. 1999). Given the complexity of NF-κB-governed biological responses, their double-edged impact on tumor development, and the inducibility of many of these responses by both oncogenes and chemotherapeutic agents, NF-κB effector functions other than anti-apoptosis are likely to contribute to impaired treatment efficacy (Li and Sethi 2010), while, in turn, not all drug-related NF-κB-controlled functions may compromise chemosensitivity.

Complementing apoptosis as a stress-inducible fail-safe mechanism, premature cellular senescence is a terminal cell cycle arrest program acutely initiated via DNA damage response (DDR) signaling evoked by oncogenic activation or anti-cancer chemotherapy (Schmitt 2007; Kuilman et al. 2010). While oncogene-induced senescence (OIS), most thoroughly studied in response to Ras/Raf-type oncogenes, imposes an anti-tumor barrier in early, (pre)-malignant lesions (Serrano et al. 1997; Braig et al. 2005), therapy-induced senescence (TIS) has been shown to improve the long-term outcome of cancer therapy (Schmitt et al. 2002). Importantly, both OIS and TIS exhibit a senescence-associated secretory phenotype (SASP) (Coppe et al. 2008), an array of predominantly proinflammatory cytokines whose autocrine or paracrine action reportedly reinforces the senescent arrest at least in some settings and whose cross-talk to the innate host immune system might explain the immune-mediated clearance of senescent tumor cells (Xue et al. 2007; Acosta et al. 2008; Kuilman et al. 2008). Many of the SASP factors are bona fide NF-κB targets with NF-κB-binding sites in their promoters (Feuerhake et al. 2005; Acosta et al. 2008; Kuilman et al. 2008), rendering them responsive to NF-κB activation, as shown for poly(ADP-ribose)-polymerase-1 (PARP-1)-mediated genotoxic therapies or induction of oncogenic Ras (Finco et al. 1997; Stilmann et al. 2009; Ohanna et al. 2011). Silencing of NF-κB transcription factors in senescent human fibroblasts enhanced their proliferative capacity, suggesting that NF-κB signaling may indeed contribute to the senescent growth arrest (Rovillain et al. 2011).

In this study, we used primary Eμ-*myc* transgenic mouse lymphomas, a well-established model for human aggressive B-cell non-Hodgkin's lymphomas (B-NHL), and information from human diffuse large B-cell lymphomas (DLBCL, the most common type of aggressive B-NHL) in a cross-species approach to identify oncogenic networks in which chemotherapy-activated NF-κB signaling no longer mediates resistance but promotes cellular senescence and contributes to the outcome of anti-cancer treatment.

Results

NF-κB activity is increased in TIS

We previously established the lymphoma-prone Eμ-*myc* transgenic mouse as a model system for TIS (Schmitt et al. 2002; Reimann et al. 2007). Primary Myc-driven B-cell lymphomas (hereafter referred to as "control" lymphomas) were isolated, underwent retroviral *bcl2* transduction to block apoptosis, and were exposed to the DNA-damaging chemotherapeutic agent adriamycin (ADR). At day 5, ADR-treated control;bcl2 lymphomas were fully growth-arrested, stained negative for the proliferation marker Ki67, and uniformly exhibited senescence-associated β-galactosidase activity (SA-β-gal) (Supplemental Fig. S1A,B; Dimri et al. 1995). To unveil TIS-related changes on the transcriptome level, we generated genome-wide microarray gene expression profiles (GEPs) from 12 matched pairs of primary control;bcl2 lymphomas that were either drug-senescent or untreated. Gene set enrichment analysis (GSEA) demonstrated that NF-κB target genes as a whole, and NF-κB-controlled cytokines in particular, were strongly skewed toward the TIS group (Fig. 1A; Supplemental Table 1). Supporting this result, a multiplex DNA-binding ELISA-based analysis of matched pairs of untreated versus senescent lymphomas detected significantly higher DNA-binding activities for the four NF-κB family subunits p50, p52, p65 (RelA), and RelB in senescent cells, indicating that both the classical and the alternative NF-κB pathways are activated in TIS (Fig. 1B). Accordingly, immunofluorescence stained p65 in TIS lymphomas predominantly in the nucleus, while nonsenescent cells displayed a preferentially cytoplasmic localization (Fig. 1C). By immunoblot analysis, TIS lymphomas also presented with induced expression levels of Ser 536-phosphorylated p65 (p65-P-S536), a post-translational modification considered to increase p65 transactivation function (Fig. 1D; Buss et al. 2004). To confirm NF-κB activity at the level of individual target genes, we measured the expression of transcripts that were among the differentially regulated gene products in the microarray analysis by quantitative real-time PCR (RQ-PCR). Indeed, all NF-κB target genes tested—non-secreted genes and SASP in particular—were expressed at higher levels in TIS compared with nonsenescent lymphoma cells (Fig. 1E). Taken together, activated NF-κB signaling is a prominent feature of chemotherapy-related senescence in full-blown tumor cells.

TIS depends on intact NF-κB function in vivo

Next, we asked whether TIS not only presents with enhanced NF-κB activity, but also depends on it. First, we tested whether inactivation of NF-κB by stable expression of the NF-κB superrepressor IκBα-ΔN (SR)—a nondegradable IκBα moiety (Krappmann et al. 1996) producing lowered expression levels of NF-κB target genes in tumor necrosis factor-α (TNF-α)-treated and little impact on proliferation in untreated lymphoma cells (Supplemental Fig. S2A,B)—is sufficient to interfere with functional properties of the TIS condition. Indeed, the expression of most NF-κB target genes—both SASP and nonsecreted genes—was sharply reduced in the ADR-exposed SR-engineered control;bcl2 lymphoma group, as further highlighted in matched-pair analyses of the same individual lymphomas with or without the SR moiety for
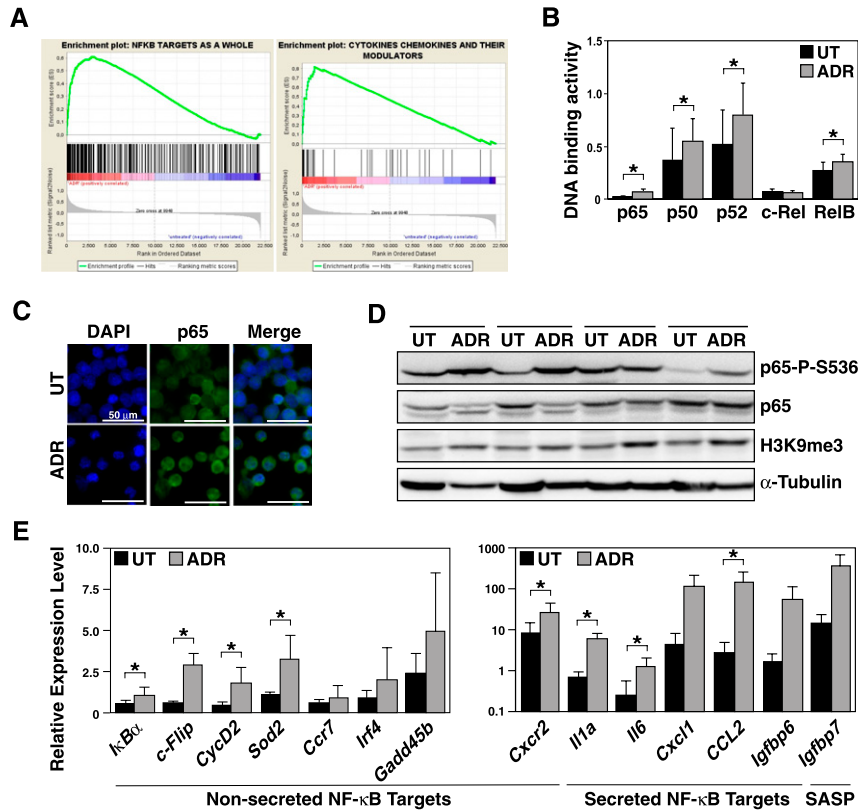
Figure 1. Enhanced NF-κB activity in therapy-induced senescent primary lymphoma cells. (*A*) GSEAs of NF-κB targets (*left*) and the subset of cytokines and their modulators therein (*right*) in the GEP of ADR senescent versus untreated (ut) Eμ-*myc* control;bcl2 lymphomas (n = 12 matched pairs). (*B*) DNA-binding activity of the indicated NF-κB subunits in lymphomas as in *A* (n ≥ 3 matched pairs per subunit). (*C*) Immunofluorescence of the NF-κB subunit p65 in cytospin preparations of lymphoma cells as in *A* (representative example of three cases analyzed; bars, 50 μm). (*D*) Immunoblot analyses of the indicated proteins in cell lysates from four matched lymphoma pairs as in *A* with H3K9me3 as a senescence marker (Reimann et al. 2010) and α-Tubulin as a loading control. (*E*) RQ-PCR analyses of the indicated nonsecreted (*left*) and secreted (*right*) transcripts in lymphomas as in *A* (n = 5 samples each). Shown are relative expression levels, normalized to an internal control, that are comparable throughout all data sets. (Note the log-scaled presentation in the cytokine panel. All secreted NF-κB targets presented here reflect SASP, while *Igfbp7* is a SASP factor, but not a bona fide NF-κB target.) All histogram bars indicate mean values ± standard deviation (SDEV).

representative NF-κB-controlled SASP factors (Fig. 2A; see Supplemental Fig. S2C for similar results obtained upon exposure to a variety of pharmacological IKK inhibitors). Based on these findings, we addressed the obvious question of whether ablation of NF-κB activity would affect the inducibility of senescence following chemotherapy. In fact, SA-β-gal-based analyses of matched pairs differing only in their SR status revealed a spectrum that reached from a substantial decline in the percentage of SA-β-gal-positive cells in some to an uncompromised TIS phenotype in other lymphomas of the SR cohort, reflecting a mean reduction of SA-β-gal reactivity by >30% and a corresponding average increase of cell numbers by >2.5-fold in the SR compared with the empty vector group (Fig. 2B; data not shown). Collectively, these data suggest a modest contribution of
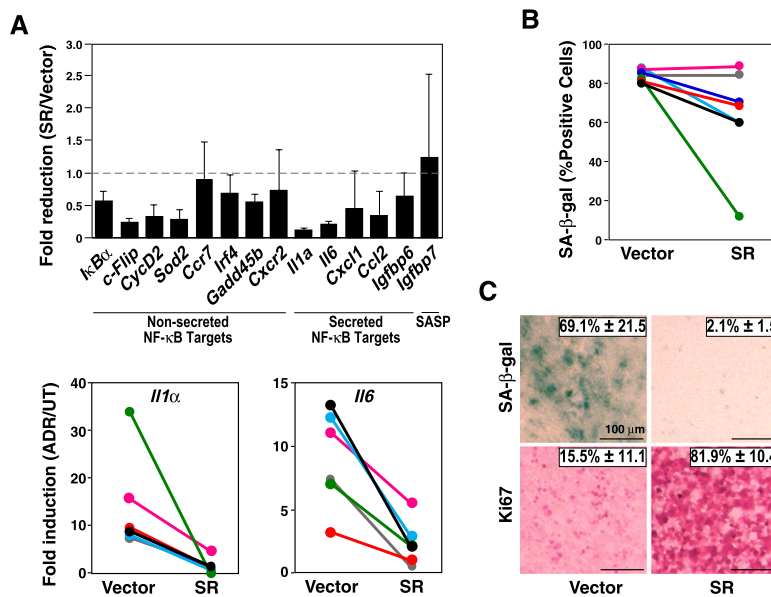

Figure 2. TIS is an NF-κB-dependent condition in primary lymphomas. (*A*, *top*) RQ-PCR analyses of the indicated transcripts in lymphomas presented as the ratio of the relative values for ADR-exposed versus untreated control;bcl2 lymphomas stably expressing the NF-κB SR or being empty vector-infected as a control (at least five samples each). (*Bottom*) Matched ADR-exposed control;bcl2 lymphoma pairs ± SR are shown for the relative expression levels of two representative SASP factors. (*B*) Frequencies of SA-β-gal-positive cells from matched lymphoma pairs ± SR, exposed to ADR in vitro (n = 7 pairs). (*C*) In situ frequencies of SA-β-gal-positive as well as Ki67-positive cells in matched-pair (±SR) lymphoma sections, exposed to CTX in vivo (n = 3 pairs; representative photomicrographs shown; bars, 100 μm). All histogram bars or numbers indicate mean values ± SDEV.

putative prosenescent NF-κB-governed functions in a homotypic tumor cell population—irrespective of their intracellular, autocrine, or paracrine modes of action (Acosta et al. 2008; Kuilman et al. 2008)—at least in a subset of genetically susceptible primary tumors. Rather than functioning as a linear and essential component of the DDR-initiated senescence pathway, it is very well conceivable that the NF-κB network operates as a corroborating, collateral relay of the prosenescent DDR. In such a scenario, the uniform exposure of all cells to a chemotherapeutic agent in culture would probably launch such a strong DDR cascade in every given cell that a quantitative reduction of a senescence-reinforcing principle by the SR will not instantly translate into a senescence-defective phenotype—except collateral prosenescent pathways became dysfunctional, thereby making the contribution of NF-κB signaling to TIS critical.

The in vivo situation is by far more complex, including aspects such as inhomogeneous drug delivery and heterotypic cell–cell interactions that were not covered by in vitro analyses. To address the potential contribution of NF-κB activity to a drug-inducible senescence phenotype in a scenario most closely recapitulating the natural tumor situation, we decided to investigate genetically compatible transplant lymphomas in vivo. Control;bcl2 lymphomas retrovirally infected with the SR construct or an empty vector for comparison were transplanted into normal, immunocompetent recipient mice, where they formed systemic lymphomas indistinguishable from the primary transgenic host they were initially derived from. At the time a peripheral lymphadenopathy became palpable, mice harboring a comparable tumor burden were treated once with the DNA-damaging anti-cancer agent cyclophosphamide (CTX), and lymphomas were analyzed for in situ signs of TIS 5 d later. Intriguingly, TIS-competent lymphomas presented with virtually no SA-β-gal reactivity and >80% Ki67-positive cells following CTX exposure in

vivo if they expressed the SR moiety (Fig. 2C). Thus, SR-expressing lymphomas displayed a much more profound TIS defect in vivo, even if they exhibited only some reduction of their SA-β-gal reactivity in vitro, indicating a critical, NF-κB-dependent prosenescent contribution of bystander cells within the tumor microenvironment. Of note, senescence-associated interaction with host immune cells is cocontrolled by NF-κB activity as well, as reported by Lowe and colleagues (Chien et al. 2011; see also Xue et al. 2007), thereby suggesting immune-mediated clearance of senescent cells as another link by which NF-κB may control tumor growth. Taken together, the NF-κB network operates as a critical component of the drug-inducible senescence response, whereby the actual quantitative impact of its interference with cell-autonomous and non-cell-autonomous senescence-relevant processes can only be appreciated in vivo.

Oncogenic networks determine opposing roles of NF-κB on treatment outcome

Given the inability of SR-engineered Myc-lymphomas to launch a TIS response in vivo, we aimed to quantify and dissect the contribution of NF-κB signaling to the long-term outcome of naturally formed B-cell lymphomas prior to any therapy. While mouse models of cancer harboring defined genetic lesions in candidate pathways are important research tools, they may miss or even disturb critical oncogenic network interactions that drive naturally developing tumors. Therefore, we started from a series of 12 primary Eμ-myc lymphomas, assessed their endogenous NF-κB activation level by p65 DNA-binding ELISA, and grouped them accordingly as an "NF-κB low" (NL, the four lowest cases) and an "NF-κB high" (NH, the four highest cases) cohort (Fig. 3A). First, we sought to determine their short-term drug sensitivity, reflecting their apoptotic potential. Expectedly, the NH group was
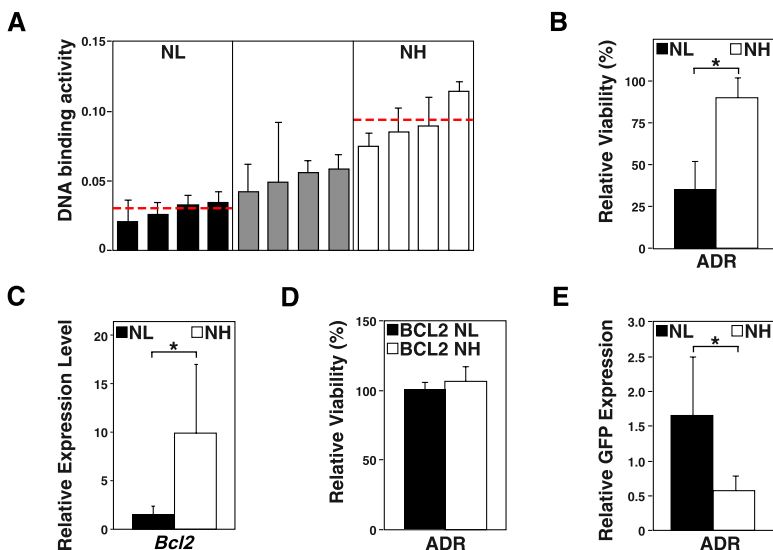

Figure 3. Eμ-myc lymphomas driven by high endogenous NF-κB levels display NF-κB/Bcl2-mediated chemoresistance. (A) Stratification of 12 primary control lymphomas in an "NF-κB low" (NL; black bars), an intermediate (gray bars), and an "NF-κB high" (NH; white bars) group according to their NF-κB p65 DNA-binding activities at diagnosis (measured in triplicate; horizontal lines indicate mean activity within the respective groups). (B) Viability analysis by trypan blue dye exclusion of the NL versus NH lymphoma cell populations exposed in vitro for 24 h to 5 ng/mL ADR relative to untreated cells of the same group (n = 4 each group). (C) RQ-PCR analyses of the transcript levels of the NF-κB target bcl2 in the lymphoma groups as in B. (D) Viability analysis as in B and with the same lymphoma samples, now overexpressing Bcl2 from retroviral alleles in both groups. (E) GFP enrichment analysis of MSCV-SR-IRES-GFP-expressing cells treated as in B, but for 48 h; selective drop of GFP-positive cells in the NH group indicating their increased chemosensitivity upon NF-κB inhibition (n = 3 each group). All histogram bars indicate mean values ± SDEV.

virtually resistant to ADR treatment in vitro, while lymphoma cells of the NL group quantitatively died at the same dose level (Fig. 3B). Since Bcl2 is frequently detected at overexpressed levels in human B-cell lymphomas and a bona fide NF-κB target, we reasoned that chemoresistance might be mediated in NH lymphomas, at least in part, via induction of Bcl2 (Schmitt et al. 2000; Feuerhake et al. 2005). Indeed, *Bcl2* transcript levels, measured by RQ-PCR, were significantly higher in the NH compared with the NL group (Fig. 3C). When we overexpressed Bcl2 from retroviral alleles in both groups, Bcl2 rendered NL lymphomas as chemoresistant as NH lymphomas (Fig. 3D). Conversely, we asked whether inhibition of NF-κB activity might overcome the short-term drug resistance in the NH group. While inactivation of NF-κB function by the SR moiety had little impact in the NL group, it restored chemosensitivity in the NH group, thereby uncovering highly active NF-κB signaling as an "Achilles' heel" of this group during chemotherapy (Fig. 3E; Staudt 2010). Taken together, a proportion of primary Myc-driven lymphomas presents with high-level NF-κB activity at diagnosis, suggestive for an oncogenic function of the NF-κB network selected for during lymphoma development that simultaneously anticipates primary drug resistance.

Recapitulating the clinical outcome of patients suffering from DLBCL, ~60% of the mice harboring Eμ-*myc* control lymphomas achieve long-term remissions (reflecting cure), while the remaining 40% encounter a relapse after CTX induction therapy (Schmitt et al. 1999, 2000; Lenz et al. 2008b). We generated "time-to-relapse" data for 13 primary (not *bcl2*-infected) Eμ-*myc* lymphomas transplanted into recipient mice and exposed to CTX at the time of lymphoma manifestation. While all animals entered a remission, seven lymphomas relapsed within the 100-d observation period, allowing us to group the 13 lymphomas

at diagnosis as either "never relapse" (NR) or "relapse-prone" (RP). Based on the previous results, we assessed basal NF-κB activity by the expression of *IκBα*, a central NF-κB regulator and NF-κB target, as well as *Bcl2* in untreated lymphomas of these two groups (Fig. 4A). Strikingly, RP lymphomas were found to exhibit significantly higher *IκBα* expression levels, further accompanied by substantially higher *bcl2* expression levels, thus reminiscent of the NF-κB/Bcl2 network analyzed in Figure 3 and of the genetic hallmark lesions detectable in activated B-cell-like (ABC) DLBCL, the prognostically inferior DLBCL subtype characterized by constitutively active NF-κB signaling due to a variety of activating mutations in the NF-κB pathway and by very high *Bcl2* transcript levels (Iqbal et al. 2006; Lenz et al. 2008b; Compagno et al. 2009; Staudt 2010; Nogai et al. 2011).

In contrast, germinal center B-cell-like (GCB) DLBCL present with a much better clinical outcome (Lenz et al. 2008b), although Bcl2 overexpression is common in this subtype as well. Importantly, GCB DLBCL rarely possess activating NF-κB mutations, but frequently (~45%) develop in the context of a t(14;18) translocation that drives Bcl2 overexpression via the immunoglobulin heavy chain locus in an NF-κB-independent fashion, a lesion that is virtually never found in ABC-type DLBCL (Nogai et al. 2011). If drug-inducible apoptosis is blocked in mouse lymphomas by exogenous Bcl2 overexpression, thereby mimicking the GCB-related t(14;18) translocation, NR lymphomas were able to enter TIS (data not shown). To test whether higher NF-κB activation levels would further promote senescence induction in these lymphomas, we made use of a strongly NF-κB-activating *CARD11* (also known as *CARMA1* or *Bimp3*) mutant, the murine homolog of the human CARD11-L244P mutant, whose overexpression results in increased NF-κB target gene
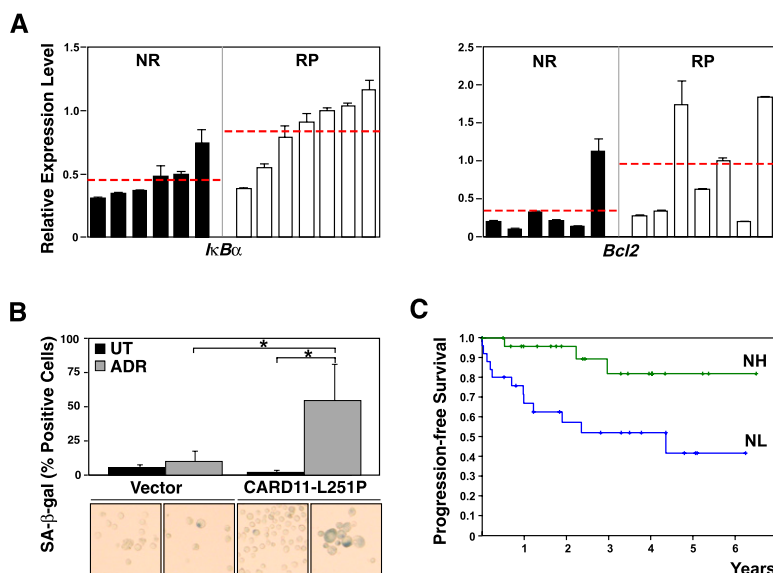

Figure 4. Differential oncogenic wiring determines opposing roles of NF-κB in treatment outcome. (*A*) Grouping of 13 primary control lymphomas according to the long-term responses to CTX therapy following transplant tumor formation in vivo as either "never relapse" (NR) or "relapse-prone" (RP) lymphomas, and RQ-PCR analyses of their *IκBα* transcript levels at diagnosis (i.e., prior to any therapy) as a representative bona fide NF-κB target (*left*) and of *Bcl2* levels of the same samples (*right*; presented in the same order); horizontal lines indicate mean activity within the respective groups. (*B*) Frequencies of SA-β-gal-positive cells in Bcl2-overexpressing NL lymphomas ± CARD11-L251P, exposed for 3 d to 50 ng/mL ADR in vitro (n = 4 matched pairs; representative photomicrographs of cytospin preparations are shown *below* the corresponding bars). (*C*) Progression-free survival of the 49 R-CHOP-like-treated GCB DLBCL patients from a total of 233 patients (as reported by Lenz et al. 2008b) with an above-median *Bcl2* expression by microarray-based transcriptome analysis of their lymphomas at diagnosis, and further stratified by a 63-gene signature as either "NF-κB high" (NH, n = 25; green) or "NF-κB low" (NL, n = 24; blue). All histogram bars indicate mean values ± SDEV.

expression (Supplemental Fig. S3; Lenz et al. 2008a). While naturally occurring *CARD11* mutations are preferentially found in ABC DLBCL, we here used such a mutant to enhance NF-κB activity in a "GCB-reminiscent" lymphoma cohort, which formed in the absence of highly activated NF-κB and where apoptosis is blocked independently of NF-κB via autochthonous Bcl2 overexpression. Indeed, at an early time, when ADR-exposed Bcl2-engineered NL lymphomas were still largely negative for signs of TIS, a high proportion of the matching, mutant CARD11-overexpressing lymphoma cells already stained positive for SA-β-gal activity (Fig. 4B), suggesting that higher NF-κB activity contributes to treatment outcome via TIS promotion.

Therefore, we decided to interrogate a large data set of DLBCL GEP and clinical data after rituximab-CHOP-like standard immunochemotherapy (which includes both ADR and CTX) from 233 patients (Lenz et al. 2008b), and asked in the subset of GCB DLBCL patients with high Bcl2 expression whether a previously identified NF-κB gene expression signature consisting of 63 known NF-κB target genes would allow us to stratify two patient cohorts with different clinical outcomes (Shaffer et al. 2006). Indeed, as shown in Figure 4C, *Bcl2*-overexpressing GCB DLBCL patients with an NF-κB signature expression above median (NH; $n = 25$) had a significantly superior progression-free survival when compared with the complementary NL group ($n = 24$; $P < 0.005$), while such a correlation was not found in patients harboring high *Bcl2*-expressing lymphomas of the ABC subtype or lymphomas of either subtype with low *Bcl2* expression (Supplemental Fig. S4; data not shown). Notably, multivariate analysis indicated that the NF-κB status in *Bcl2*-overexpressing GCB DLBCL cases is statistically independent of the International Prognostic Index overall score ($P = 0.3956$), which is used as a clinical standard to predict outcome in lymphoma patients (The International Non-Hodgkin's Lymphoma Prognostic Factors Project 1993). Taken together, our experimental strategy led to the identification of a genetically defined and clinically significant subgroup of GCB DLBCL patients who experienced superior treatment outcome if NF-κB signaling was hyperactive, thereby contrasting the well-established association of the ABC subtype with constitutively active NF-κB signaling and poor treatment outcome.

Discussion

Cellular senescence not only acts as a tumor-suppressive principle, but contributes to the outcome of cancer therapy in vivo (Schmitt et al. 2002; Haugstetter et al. 2010). Activated NF-κB signaling has mostly been linked to treatment resistance, especially when measured as inability to enter drug-induced apoptosis in short-term assays (Wang et al. 1999). As suggested by previous studies linking OIS to the massive production of a large variety of cytokines of which many possess NF-κB-binding sites in their promoters, we report here a dramatic induction of nonsecreted and secreted NF-κB target genes during TIS and, importantly, a dependency of the senescent phenotype on functional NF-κB signaling that becomes particularly

evident in vivo—a finding in full agreement with related work by Lowe and colleagues in this issue (Chien et al. 2011). While enforced NF-κB activation due to mutant Card11 expression accelerated TIS in vitro, the much more pronounced impairment of TIS following NF-κB inhibition in vivo as compared with the in vitro situation indicates additional, non-cell-autonomous implications of NF-κB signaling in the senescence process. Our observation of a virtual absence of senescence in NF-κB-defective lymphoma cells at a time when NF-κB-competent lymphomas became largely senescent argues for prosenescent factors released by adjacent cells in response to NF-κB-dependent signals originating from the treated tumor cells, reminiscent of the non-cell-autonomous mode of senescence induction recently reported for macrophages during Eμ-*myc* lymphomagenesis (Reimann et al. 2010).

Although our results demonstrate an essential role for NF-κB in the induction of cellular senescence in a genetically defined model scenario, the overall impact of NF-κB activity levels on treatment outcome in natural tumors is much more difficult to assess. Our cross-species investigation strategy was instrumental in unveiling a genetically defined tumor subset with a distinct NF-κB-dependent responsiveness. Based on human DLBCL data linking the ABC subtype to activating NF-κB lesions and an inferior outcome to standard immunochemotherapy (Lenz et al. 2008b; Compagno et al. 2009), we first classified a series of primary Eμ-*myc* transgenic lymphomas with known long-term responses to chemotherapy in vivo based on their NF-κB activity levels at manifestation. Reminiscent of GCB-type DLBCL, the group of Eμ-*myc* lymphomas with good clinical outcome was largely composed of lymphomas exhibiting low basal NF-κB activity. These mouse lymphomas were subsequently used to experimentally explore the contribution of enhanced NF-κB activity to senescence induction after drug-inducible apoptosis was independently blocked by retroviral Bcl2 overexpression. Ultimately, we used the genetic determinants of this TIS-prone scenario—GCB-reminiscent lymphomas with high *Bcl2* expression and high NF-κB activity—to interrogate a large GEP set derived from 233 DLBCL patients with known clinical outcome to therapy. Strikingly, we were able to confirm the mechanistic results from the murine lymphoma model in DLBCL-harboring patients. The "*Bcl2* high/ NF-κB high" GCB DLBCL subgroup of patients presenting with a significantly prolonged survival after therapy underscores a hitherto unknown beneficial association of NF-κB hyperactivation and treatment outcome in lymphoma patients and would not have been identified without the cross-species investigation of primary Eμ-*myc* lymphomas. Our approach illustrates the power of mouse models to recapitulate defined genetic determinants of human tumor cohorts, followed by the genetic manipulation and subsequent functional exploration of murine surrogate tumors with the ultimate goal to use mouse-derived mechanistic information for a reassessment of the human data set to gain novel functional insights.

Our data highlight how oncogenic networks and interdependencies, wired up during tumor development,

may regulate the actual functions and even opposing roles of NF-κB in subsequent responses to therapy. NF-κB mutations acquired during lymphoma development, as preferentially observed in the ABC subtype of DLBCL, account for the selective vulnerability of these lymphomas to NF-κB inhibitors or shRNAs targeting components of the NF-κB pathway (Davis et al. 2001; Ngo et al. 2006). Since the anti-apoptotic *bcl2* gene is a bona fide NF-κB target, ABC DLBCLs are genetically determined to depend on an NF-κB/Bcl2 signaling module, while GCB DLBCLs frequently present with *bcl2* translocations that uncouple their anti-apoptotic activity from NF-κB upstream control. Unlike tumors characterized by a broad spectrum of detrimental biological properties directly linked to their constitutively active NF-κB network, tumor types that do not rely on NF-κB signaling as the driving oncogenic force but present with an NF-κB-independent apoptotic block may use the prosenescent potential of NF-κB signaling to execute TIS as an alternative, outcome-improving chemotherapeutic effector mechanism. Our mouse model findings obtained in Myc-driven lymphomas engineered to overexpress Bcl2 not only genetically approximate the human Myc/Bcl2 "double-hit" lymphomas most frequently found in the GCB subtype of DLBCL, but also more advanced follicular lymphomas, which, in addition to their t(14;18) hallmark lesion, often acquire activating Myc lesions in the course of the disease, and, of note, also do not belong to NF-κB-hyperactivated lymphoma entities (Aukema et al. 2011). Although NF-κB's role in cancer development and therapy is very complex, our mouse model– and patient-derived data suggest that we should carefully select, or at least monitor, genetically defined patient subcohorts in which therapeutic interference with the NF-κB pathway may or may not be of clinical benefit (Dunleavy et al. 2009; Ruan et al. 2011).

Materials and methods

Mice, lymphoma monitoring, and in vivo treatment

All animal protocols used in this study were approved by the governmental review board (Landesamt Berlin) and conform to the respective regulatory standards. Eµ-*myc* transgenic mice were genotyped by allele-specific genomic PCR and monitored for lymphoma onset (Adams et al. 1985; Schmitt et al. 1999). Viable lymphoma cells were isolated, transplanted by tail vein injection into strain-matched C57BL/6 recipient mice ($\sim3\times 10^6$ to 5×10^6 cells per mouse), or propagated in culture, and preservation of snap-frozen or formalin-fixed lymph node tissue was carried out as described (Schmitt et al. 1999). At the moment lymph nodes became palpable in recipient animals, mice were exposed to a single intraperitoneal dose of CTX (300 mg/kg body weight), and responses were monitored by lymph node palpation or in lymphoma material isolated at day 5 after therapy (Schmitt et al. 1999, 2002).

Site-directed mutagenesis, plasmids, and retroviral gene transfer

The oncogenic CARD11-L251P mutation (the murine homolog of the human CARD11-L244P mutation detected in the ABC DLBCL cell line OCL-Ly3) (Lenz et al. 2008a) was generated by site-directed mutagenesis of full-length wild-type murine CARD11 (BioCat). cDNAs encoding murine wild-type CARD11, CARD11-L251P, Bcl2, and the NF-κB SR (Krappmann et al. 1996) were subcloned into the murine stem cell retrovirus (MSCV; i.e., into MSCV-IRES-GFP or MSCV backbones coexpressing a blasticidin or puromycin antibiotic resistance gene). Retroviral supernatants, generated by transient transfections of Phoenix packaging cells with the respective MSCV plasmids, were used to stably infect Eµ-*myc* transgenic lymphoma cells as described (Schmitt et al. 2000).

Growth parameters and in vitro drug assays

Cell numbers and cellular viability were assessed by trypan blue dye exclusion, and cytotoxicity or cellular senescence was measured 24 h or 5 d, respectively, after the addition of ADR at the indicated concentrations (Schmitt et al. 1999; Reimann et al. 2010). In some experiments, lymphoma cells were pre-exposed for 30 min to the pharmacological NF-κB inhibitors Bay11-7082 (1 µM; an IκBα phosphorylation inhibitor; Sigma-Aldrich), TPCA-1 (0.5 µM; an IKK-2 inhibitor; Merck), an IKK-2 inhibitor; kindly provided by M. Schmidt-Supprian [Schon et al. 2008]) prior to a subsequent ADR treatment, or were treated with TNF-α (Sigma-Aldrich) at 50 µM for 30 min or 24 h. For GFP enrichment analyses of MSCV-SR-IRES-GFP-infected cells, changes in the percentage of GFP-positive cells prior to and after ADR exposure were normalized by the respective fractions of GFP-positive cells infected with an MSCV-GFP control vector. Cytospin preparations of suspension cultures for subsequent antigen- or SA-β-gal activity-detecting staining as well as in situ-SA-β-gal analyses in cryosections of snap-frozen lymph nodes were carried out as previously described (Schmitt et al. 2002; Braig et al. 2005; Reimann et al. 2010).

NF-κB DNA-binding activity

DNA-binding activity of the five mammalian NF-κB subunits was measured using the TransAm Flexi NFκB Family transcription factor ELISA assay (Active Motif) in accordance with the manufacturer's protocol.

Gene expression analyses

For RQ-PCR analyses of NF-κB target genes in lymphoma cells, RNA extracted with TRIzol (Invitrogen) was transcribed into cDNA using SuperScript reverse transcriptase (Invitrogen) and random hexamers or oligo-dT. RQ-PCR analyses of murine *Bcl2*, *CCL2*, *CCR7*, *c-FLIP*, *CXCL1*, *CXCR2*, *Cyclin D2*, *GADD45b*, *GAPDH*, *GM-CSF*, *IGFBP6*, *IGFBP7*, *IκBα*, *IL-1α*, *IL-6*, *IRF-4*, and *SOD2* transcripts were conducted based on commercially available primers (Applied Biosystems). For every given sample, ΔCt values were determined as the difference between the Ct value of a specific transcript and the Ct value of *GAPDH*, serving as the housekeeping control mRNA, and relative transcript levels (e.g., treated vs. untreated) were then produced based on $2^{(-\Delta\Delta Ct)}$ with $\Delta\Delta Ct = \Delta Ct_{treated} - \Delta Ct_{untreated}$.

Immunoblotting was carried out using whole-cell lysates, generated by lysing cells in sodium dodecyl sulfate (SDS) sample buffer (60 mM Tris-HCl at pH 6.8, 10% glycerol, 2% SDS, and 5% 2-mercaptoethanol), resolved on a 12% SDS-PAGE, and transferred to an Immobilon-P membrane (Millipore) using antibodies against Bcl2 (1:2000 dilution; #554087, BD Pharmingen) (data not shown), H3K9me3 (1:1000; ab8898, Abcam), NF-κB p65 (1:1000; #3034, Cell Signaling Technology), NF-κB p65-P-S536 (1:1000; #3033, Cell Signaling Technology), and α-Tubulin (1:2500;

T5168, Sigma) as a loading control (Schmitt et al. 1999). For immunofluorescence, cells were fixed in 4% paraformaldehyde, permeabilized with 0.1% Triton X-100/PBS, blocked in 1% bovine serum albumin, and incubated with a primary antibody against p65 (1:250; Santa Cruz Biotechnologies, SC-372), followed by 0.01% Tween 20 as detergent buffer and the secondary anti-rabbit IgG antibody (1:400; AlexaFluor 488 [A11008], Invitrogen); slides were stained with DAPI (4′,6-diamidino-2-phenyl-indole) as a nuclear counterstain and mounted with Mowiol 4-88 (Calbiochem). For immunostaining of Ki67, 2% paraformalde-hyde-fixed cytospin preparations or tissue cryosections were incubated with the primary antibody against Ki67 (1:25; M7240, Dako), followed by a streptavidin–biotin complex peroxidase kit (LSAB+ System-AP, DakoCytomation), used according to the manufacturer's instructions.

For microarray-based gene expression profiling, RNA was isolated from untreated or 5-d ADR-treated control;bcl2 Eμ-*myc* lymphomas using the RNeasy minikit (Qiagen) and hybridized to Affymetrix Mouse Genome 430 2.0 microarrays (Affymetrix) according to the manufacturer's instructions. The arrays were hybridized and washed in the GeneChip Fluidics Station 450, and signals were detected on an Affymetrix GeneChip Scanner 3000. Affymetrix files were imported into Partek Genomic Suite software (version 6.4, Partek, Inc.) and processed by the implemented robust multiarray (RMA) work flow (consisting of median polish probe set summarization, RMA background correction, and quantile normalization). The raw microarray data were deposited at the Gene Expression Omnibus (GEO) repository of the National Center for Biotechnology Information under the accession number GSE31099 (http://www.ncbi.nlm.nih.gov/geo/query/acc.cgi?acc=GSE31099).

For further analysis of mouse microarray data, genetic signatures of NF-κB activation were taken without further change from the Thomas Gilmore laboratory Web site (a complete list of genes and related references is available at http://www.bu.edu/nf-kb/gene-resources/target-genes). The enrichment of NF-κB target gene sets within the global transcript signals from matched pairs of untreated versus ADR-treated control;bcl2 lymphoma cells was analyzed by applying the GSEA version 2.0 software (Broad Institute of the Massachusetts Institute of Technology and Harvard, http://www.broad.mit.edu/gsea). Normalized enrichment scores (NES) reflect a statistically significant enrichment for P-values <0.05 and FDR (false discovery rate) values <0.25 (Subramanian et al. 2005).

Gene expression data of lymphoma biopsies from 233 patients, who were treated with R-CHOP-like immunochemotherapy and profiled using Affymetrix HG-U133 Plus 2.0 microarrays (Lenz et al. 2008b), were obtained from the NCBI GEO (GSE10846). Patients were classified into ABC DLBCL, GCB DLBCL, and unclassified DLBCL according to Lenz et al. (2008b). The 100 GCB DLBCL patient samples, for which clinical follow-up information for progression-free survival was available, were equally divided into groups of high and low *Bcl2* expression, based on the median expression. Within these two cohorts, patients were subsequently divided into high and low NF-κB groups according to the median expression of a previously described NF-κB gene expression signature consisting of 63 known NF-κB target genes (http://lymphochip.nih.gov/cgi-bin/signaturedb/signatureDB_DisplayGenes.cgi?signatureID=83; Shaffer et al. 2006).

Statistical evaluation

The survival of GEP-related patient subcohorts was calculated using Kaplan-Meier estimation and compared with the log-rank (Mantel-Cox) test. Pearson's χ^2-test was applied in multivariate analysis. The unpaired t-test was used to compare means and

standard deviations. All quantifications from staining reactions (i.e., immunostainings or SA-β-gal assays) were carried out by an independent and blinded second examiner and reflect at least three samples with at least 200 events counted (typically in more than three different areas) each. A P-value <0.05 was considered statistically significant and was marked by an asterisk.

References

Acosta JC, O'Loghlen A, Banito A, Guijarro MV, Augert A, Raguz S, Fumagalli M, Da Costa M, Brown C, Popov N, et al. 2008. Chemokine signaling via the CXCR2 receptor reinforces senescence. *Cell* **133:** 1006–1018.

Adams JM, Harris AW, Pinkert CA, Corcoran LM, Alexander WS, Cory S, Palmiter RD, Brinster RL. 1985. The c-*myc* oncogene driven by immunoglobulin enhancers induces lymphoid malignancy in transgenic mice. *Nature* **318:** 533–538.

Aukema SM, Siebert R, Schuuring E, van Imhoff GW, Kluin-Nelemans HC, Boerma EJ, Kluin PM. 2011. Double-hit B-cell lymphomas. *Blood* **117:** 2319–2331.

Basseres DS, Ebbs A, Levantini E, Baldwin AS. 2010. Requirement of the NF-κB subunit p65/RelA for K-Ras-induced lung tumorigenesis. *Cancer Res* **70:** 3537–3546.

Ben-Neriah Y, Karin M. 2011. Inflammation meets cancer, with NF-κB as the matchmaker. *Nat Immunol* **12:** 715–723.

Brach MA, Hass R, Sherman ML, Gunji H, Weichselbaum R, Kufe D. 1991. Ionizing radiation induces expression and binding activity of the nuclear factor κB. *J Clin Invest* **88:** 691–695.

Braig M, Lee S, Loddenkemper C, Rudolph C, Peters AH, Schlegelberger B, Stein H, Dorken B, Jenuwein T, Schmitt CA. 2005. Oncogene-induced senescence as an initial barrier in lymphoma development. *Nature* **436:** 660–665.

Buss H, Dorrie A, Schmitz ML, Hoffmann E, Resch K, Kracht M. 2004. Constitutive and interleukin-1-inducible phosphorylation of p65 NF-κB at serine 536 is mediated by multiple protein kinases including IκB kinase (IKK)-α, IKKβ, IKKε, TRAF family member-associated (TANK)-binding kinase 1 (TBK1), and an unknown kinase and couples p65 to TATA-binding protein-associated factor II31-mediated interleukin-8 transcription. *J Biol Chem* **279:** 55633–55643.

Calado DP, Zhang B, Srinivasan L, Sasaki Y, Seagal J, Unitt C, Rodig S, Kutok J, Tarakhovsky A, Schmidt-Supprian M, et al. 2010. Constitutive canonical NF-κB activation cooperates with disruption of BLIMP1 in the pathogenesis of activated B cell-like diffuse large cell lymphoma. *Cancer Cell* **18:** 580–589.

Chien Y, Scuoppo C, Wang X, Fang X, Balgley B, Bolden JE, Premsrirut P, Luo W, Chicas A, Lee CS, et al. 2011. Control of the senescence-associated secretory phenotype by NF-kB promotes senescence and enhances chemosensitivity. *Genes Dev* (this issue). doi: 10.1101/gad.17276711.

Compagno M, Lim WK, Grunn A, Nandula SV, Brahmachary M, Shen Q, Bertoni F, Ponzoni M, Scandurra M, Califano A, et al. 2009. Mutations of multiple genes cause deregulation of NF-κB in diffuse large B-cell lymphoma. *Nature* **459:** 717–721.

Coppe JP, Patil CK, Rodier F, Sun Y, Munoz DP, Goldstein J, Nelson PS, Desprez PY, Campisi J. 2008. Senescence-associated secretory phenotypes reveal cell-nonautonomous functions of oncogenic RAS and the p53 tumor suppressor. *PLoS Biol* **6:** 2853–2868.

Davis RE, Brown KD, Siebenlist U, Staudt LM. 2001. Constitutive nuclear factor κB activity is required for survival of activated B cell-like diffuse large B cell lymphoma cells. *J Exp Med* **194:** 1861–1874.

Dimri GP, Lee X, Basile G, Acosta M, Scott G, Roskelley C, Medrano EE, Linskens M, Rubelj I, Pereira-Smith O, et al. 1995. A biomarker that identifies senescent human cells in culture and in aging skin in vivo. *Proc Natl Acad Sci* **92:** 9363–9367.

Dunleavy K, Pittaluga S, Czuczman MS, Dave SS, Wright G, Grant N, Shovlin M, Jaffe ES, Janik JE, Staudt LM, et al. 2009. Differential efficacy of bortezomib plus chemotherapy within molecular subtypes of diffuse large B-cell lymphoma. *Blood* **113:** 6069–6076.

Feuerhake F, Kutok JL, Monti S, Chen W, LaCasce AS, Cattoretti G, Kurtin P, Pinkus GS, de Leval L, Harris NL, et al. 2005. NFκB activity, function, and target-gene signatures in primary mediastinal large B-cell lymphoma and diffuse large B-cell lymphoma subtypes. *Blood* **106:** 1392–1399.

Finco TS, Westwick JK, Norris JL, Beg AA, Der CJ, Baldwin AS Jr. 1997. Oncogenic Ha-Ras-induced signaling activates NF-κB transcriptional activity, which is required for cellular transformation. *J Biol Chem* **272:** 24113–24116.

Haugstetter AM, Loddenkemper C, Lenze D, Grone J, Standfuss C, Petersen I, Dorken B, Schmitt CA. 2010. Cellular senescence predicts treatment outcome in metastasised colorectal cancer. *Br J Cancer* **103:** 505–509.

Hayden MS, Ghosh S. 2008. Shared principles in NF-κB signaling. *Cell* **132:** 344–362.

Hinz M, Stilmann M, Arslan SC, Khanna KK, Dittmar G, Scheidereit C. 2010. A cytoplasmic ATM–TRAF6–cIAP1 module links nuclear DNA damage signaling to ubiquitin-mediated NF-κB activation. *Mol Cell* **40:** 63–74.

The International Non-Hodgkin's Lymphoma Prognostic Factors Project. 1993. A predictive model for aggressive non-Hodgkin's lymphoma. *N Engl J Med* **329:** 987–994.

Iqbal J, Neppalli VT, Wright G, Dave BJ, Horsman DE, Rosenwald A, Lynch J, Hans CP, Weisenburger DD, Greiner TC, et al. 2006. BCL2 expression is a prognostic marker for the activated B-cell-like type of diffuse large B-cell lymphoma. *J Clin Oncol* **24:** 961–968.

Keller U, Huber J, Nilsson JA, Fallahi M, Hall MA, Peschel C, Cleveland JL. 2010. Myc suppression of Nfkb2 accelerates lymphomagenesis. *BMC Cancer* **10:** 348. doi: 10.1186/1471-2407-10-348.

Krappmann D, Wulczyn FG, Scheidereit C. 1996. Different mechanisms control signal-induced degradation and basal turnover of the NF-κB inhibitor IκBα in vivo. *EMBO J* **15:** 6716–6726.

Kuilman T, Michaloglou C, Vredeveld LC, Douma S, van Doorn R, Desmet CJ, Aarden LA, Mooi WJ, Peeper DS. 2008. Oncogene-induced senescence relayed by an interleukin-dependent inflammatory network. *Cell* **133:** 1019–1031.

Kuilman T, Michaloglou C, Mooi WJ, Peeper DS. 2010. The essence of senescence. *Genes Dev* **24:** 2463–2479.

Lenz G, Davis RE, Ngo VN, Lam L, George TC, Wright GW, Dave SS, Zhao H, Xu W, Rosenwald A, et al 2008a. Oncogenic CARD11 mutations in human diffuse large B cell lymphoma. *Science* **319:** 1676–1679.

Lenz G, Wright G, Dave SS, Xiao W, Powell J, Zhao H, Xu W, Tan B, Goldschmidt N, Iqbal J, et al 2008b. Stromal Gene signatures in large-B-cell lymphomas. *N Engl J Med* **359:** 2313–2323.

Li F, Sethi G. 2010. Targeting transcription factor NF-κB to overcome chemoresistance and radioresistance in cancer therapy. *Biochim Biophys Acta* **1805:** 167–180.

Luedde T, Beraza N, Kotsikoris V, van Loo G, Nenci A, De Vos R, Roskams T, Trautwein C, Pasparakis M. 2007. Deletion of NEMO/IKKγ in liver parenchymal cells causes steatohepatitis and hepatocellular carcinoma. *Cancer Cell* **11:** 119–132.

Ngo VN, Davis RE, Lamy L, Yu X, Zhao H, Lenz G, Lam LT, Dave S, Yang L, Powell J, et al. 2006. A loss-of-function RNA interference screen for molecular targets in cancer. *Nature* **441:** 106–110.

Nogai H, Dorken B, Lenz G 2011. Pathogenesis of non-Hodgkin's lymphoma. *J Clin Oncol* **29:** 1803–1811.

Ohanna M, Giuliano S, Bonet C, Imbert V, Hofman V, Zangari J, Bille K, Robert C, Bressac-de Paillerets B, Hofman P, et al. 2011. Senescent cells develop a PARP-1 and nuclear factor-κB-associated secretome (PNAS). *Genes Dev* **25:** 1245–1261.

Perkins ND, Gilmore TD. 2006. Good cop, bad cop: the different faces of NF-κB. *Cell Death Differ* **13:** 759–772.

Reimann M, Loddenkemper C, Rudolph C, Schildhauer I, Teichmann B, Stein H, Schlegelberger B, Dorken B, Schmitt CA. 2007. The Myc-evoked DNA damage response accounts for treatment resistance in primary lymphomas in vivo. *Blood* **110:** 2996–3004.

Reimann M, Lee S, Loddenkemper C, Dörr JR, Tabor V, Aichele P, Stein H, Dörken B, Jenuwein T, Schmitt CA. 2010. Tumor stroma-derived TGF-β limits Myc-driven lymphomagenesis via Suv39h1-dependent senescence. *Cancer Cell* **17:** 262–272.

Rovillain E, Mansfield L, Caetano C, Alvarez-Fernandez M, Caballero OL, Medema RH, Hummerich H, Jat PS. 2011. Activation of nuclear factor-κB signalling promotes cellular senescence. *Oncogene* **30:** 2356–2366.

Ruan J, Martin P, Furman RR, Lee SM, Cheung K, Vose JM, Lacasce A, Morrison J, Elstrom R, Ely S, et al. 2011. Bortezomib plus CHOP-rituximab for previously untreated diffuse large B-cell lymphoma and mantle cell lymphoma. *J Clin Oncol* **29:** 690–697.

Ryan KM, Ernst MK, Rice NR, Vousden KH. 2000. Role of NF-κB in p53-mediated programmed cell death. *Nature* **404:** 892–897.

Schmitt CA. 2007. Cellular senescence and cancer treatment. *Biochim Biophys Acta* **1775:** 5–20.

Schmitt CA, McCurrach ME, de Stanchina E, Wallace-Brodeur RR, Lowe SW. 1999. INK4a/ARF mutations accelerate lymphomagenesis and promote chemoresistance by disabling p53. *Genes Dev* **13:** 2670–2677.

Schmitt CA, Rosenthal CT, Lowe SW. 2000. Genetic analysis of chemoresistance in primary murine lymphomas. *Nat Med* **6:** 1029–1035.

Schmitt CA, Fridman JS, Yang M, Lee S, Baranov E, Hoffman RM, Lowe SW. 2002. A senescence program controlled by p53 and p16INK4a contributes to the outcome of cancer therapy. *Cell* **109:** 335–346.

Schon M, Wienrich BG, Kneitz S, Sennefelder H, Amschler K, Vohringer V, Weber O, Stiewe T, Ziegelbauer K, Schon MP. 2008. KINK-1, a novel small-molecule inhibitor of IKKβ, and the susceptibility of melanoma cells to antitumoral treatment. *J Natl Cancer Inst* **100:** 862–875.

Sen R, Baltimore D. 1986. Multiple nuclear factors interact with the immunoglobulin enhancer sequences. *Cell* **46:** 705–716.

Serrano M, Lin AW, McCurrach ME, Beach D, Lowe SW. 1997. Oncogenic ras provokes premature cell senescence associated with accumulation of p53 and p16INK4a. *Cell* **88:** 593–602.

Shaffer AL, Wright G, Yang L, Powell J, Ngo V, Lamy L, Lam LT, Davis RE, Staudt LM. 2006. A library of gene expression signatures to illuminate normal and pathological lymphoid biology. *Immunol Rev* **210:** 67–85.

Staudt LM. 2010. Oncogenic activation of NF-κB. *Cold Spring Harb Perspect Biol* **2:** a000109. doi: 10.1101/cshperspect. a000109.

Stilmann M, Hinz M, Arslan SC, Zimmer A, Schreiber V, Scheidereit C. 2009. A nuclear poly(ADP-ribose)-dependent signalosome confers DNA damage-induced IκB kinase activation. *Mol Cell* **36:** 365–378.

Subramanian A, Tamayo P, Mootha VK, Mukherjee S, Ebert BL, Gillette MA, Paulovich A, Pomeroy SL, Golub TR, Lander ES, et al. 2005. Gene set enrichment analysis: a knowledge-based approach for interpreting genome-wide expression profiles. *Proc Natl Acad Sci* **102:** 15545–15550.

Wang CY, Mayo MW, Korneluk RG, Goeddel DV, Baldwin AS Jr. 1998. NF-κB antiapoptosis: induction of TRAF1 and TRAF2 and c-IAP1 and c-IAP2 to suppress caspase-8 activation. *Science* **281:** 1680–1683.

Wang CY, Cusack JC Jr, Liu R, Baldwin AS Jr. 1999. Control of inducible chemoresistance: enhanced anti-tumor therapy through increased apoptosis by inhibition of NF-κB. *Nat Med* **5:** 412–417.

Xue W, Zender L, Miething C, Dickins RA, Hernando E, Krizhanovsky V, Cordon-Cardo C, Lowe SW. 2007. Senescence and tumour clearance is triggered by p53 restoration in murine liver carcinomas. *Nature* **445:** 656–660.

Yang J, Splittgerber R, Yull FE, Kantrow S, Ayers GD, Karin M, Richmond A. 2010. Conditional ablation of Ikkb inhibits melanoma tumor development in mice. *J Clin Invest* **120:** 2563–2574.